Low Cost Wideband Digital Beamforming

Divaydeep Sikri
SatixFy UK Ltd., 279 Farnborough Road, Farnborough, UK GU14 7LS,
Tel: +44-1252547665,
sikri.divaydeep@satixfy.com
Bahadir Canpolat
SatixFy UK Ltd., 279 Farnborough Road, Farnborough, UK GU14 7LS,
Tel: +44-1252547665,
bahadir.canpolat@satixfy.com
Cetin Altan
SatixFy UK Ltd., 279 Farnborough Road, Farnborough, UK GU14 7LS,
Tel: +44-1252547665,
cetin.altan@satixfy.com

Abstract

In a previous paper, [1], the structure and architecture of a fully digital wideband beamforming array was introduced. In this paper, we analyze the performance and limits of such an antenna array taking into account actual implementation.
TTD performance, impact of impairments (phase noise, random phase and gain errors), grating lobes, and equalization for wideband operation.
The paper analyzes the errors and impairments introduced by the above effects, and shows the feasibility of a fully digital design for a variety of applications in the satellite communication field.

1. Introduction

As we usher into an age of large capacity wireless access systems demanding high spectral efficiencies, array antennas are playing an ever-increasing role in radio and wireless communication system. Multi-Input Multi-Output (MIMO) antenna arrays has now become an integral part of the standards for cellular and wireless local area networks in current and future generations [11]. These active antenna arrays will play an equally important role in next generation high throughput-satellite (HTS) communications. Also with introduction of large LEO and MEO constellations being planned by companies like OneWeb, O3b and SpaceX, there will be a growing need for antennas at ground terminals tracking multiple satellites. The parabolic dish antennas have been de-facto satcom earth antenna thus far because of mostly fixed pointing for GSO applications. These antennas have their advantages from cost and power consumption but also are extremely inflexible and have lower efficiencies. On the other hand, electronically steerable antennas are active scanning antennas that provide many benefit viz self-installation capabilities, multi-satellite communication and satellite tracking. Payloads can be made more flexible and enable techniques such as multibeam, beam hopping and flexible beam shaping. All - electronic control removes the need for moving mechanical parts, which are slow and more prone to malfunctions.

In this paper, we present true-time delay digital beamformer solution with performance analysis. This chip set is being developed in Satixfy, with support from the European Space Agency. While analog techniques for phase arrays are now mature and provide good solutions, the digital solution is, in our opinion, more viable and flexible and also suitable for wide bandwidth applications. The paper is organized as follows: Section 2 of the paper deals with topic of True Time Delay and its prominent role in the wideband application. While antenna bandwidth is a function of antenna's effective aperture, for an array the spacing between the antenna elements contribute to effects such as mutual coupling and grating lobes. Section 3 deals with this topic with focus on grating lobes. Section 4 introduces some of the analog and digital impairments and their impact on the array performance. Finally, Section 5 extends into providing a short insight into calibration by putting forward a simple model that captures various contributors to phase and delay for a digital beamformer implementation as well as an overview of RF Front End equalizer.

2. True Time Delay Digital Beamformer

To begin with, we will consider a Uniform Linear Array (ULA) as shown below and the analysis shown below can be easily extended to Planar Arrays and Conformal antenna arrays.

Uniform linear array structure

Figure 1 below shows Uniform Linear Array with N elements stacked in 1-D with wavefront incident on this ULA at an angle θ. The incidence angle results in a delay in signal arrival at different elements w.r.t each other.

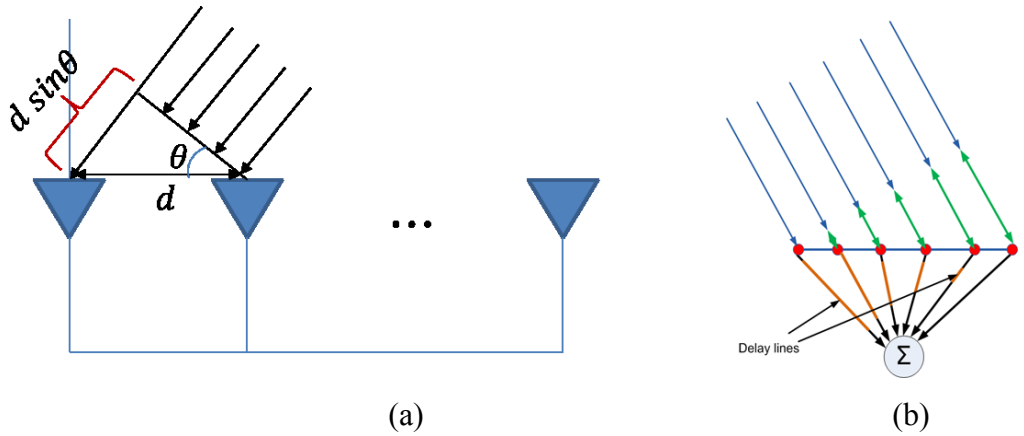

(a) (b)

Figure 1- (a) Uniform Linear Array with wavefront incident at an angle $\boldsymbol{\theta}$
(b) in TTD technology additional "delay lines" to compensate for the resulting delays

Let the signal received at the n[th] element of the antenna array be given as

$$y_n(t) = x(t + n\tau)exp\big(j2\pi f_c(t + n\tau)\big) \quad [2.1]$$

where, $y_n(t)$ is the received signal at n[th] element

$x(t)$ is the baseband signal that is modulated by the carrier frequency f_c

τ is the delay between the two adjacent elements of the array

d is the distance between two elements assumed to be $\lambda/2$

The delay τ in the expression above is related to the angle of incidence of wavefront as shown below:

$$\tau = \frac{sin\theta}{2f_c} \quad [2.2]$$

The delay is minimal for boresight and maximal in the end-fire direction for which θ is 90°

$$\text{Boresight: } \tau = 0$$

$$\text{Endfire: } \tau = \frac{1}{2f_c}$$

Impact of the delay

From equation [2.1], for the last antenna element N, the signal received is given as:

$$y_N(t) = x(t + N\tau)exp\big(j2\pi f_c(t + N\tau)\big) \quad [2.3]$$

Now it can be observed that delay results in phase offset as well as a delay in the baseband signal.
As long as the baseband signal is narrowband or if the antenna is small, then the following approximation

holds

$$\boldsymbol{x(t+N\tau) \sim x(t)}, \text{ for } \boldsymbol{N\tau \ll T_s = \frac{1}{BW}} \quad [2.4]$$

If the above expression is not true, then the delay in baseband signal cannot be ignored and if uncorrected contributes to frequency selective fading or inter-symbol interference.

Phase array versus TTD

The following is an example of beamformed expression where the only phase has been corrected, and in the other, both phase and delay have been compensated.

Phased Array:

$$y_B(t) = \sum_{n=0}^{N-1} y_n(t)\exp(-j\varphi_n) \quad [2.5]$$

True Time Delay:

$$y_B(t) = \sum_{n=0}^{N-1} y_n(t-\tau_n)\exp(-j\varphi_n) \quad [2.6]$$

From the equation above, the True Time Delay system can be considered as delay lines added in addition to phase offsets to correct for delay and phase (*Figure 1*).

For a wideband signal e.g. composed of 3 tones 19GHz, 20GHz and 21GHz incident on the ULA at angle 20°, the Phased Array will result in beam squint as shown in **Figure 2** below.

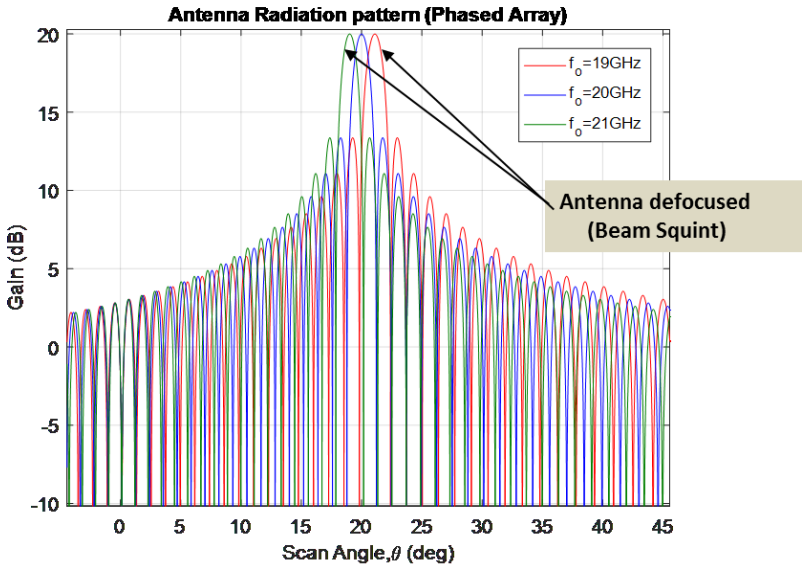

Figure 2 - Antenna Radiation pattern for Phased Array showing Beam squint

Beam squint causes antenna defocussing whereby antenna gain becomes frequency dependent. Hence wideband signals are susceptible to Beam Squints in Phased Array implementation.

On the other hand, the True Time Delay, which corrects for both Delay and Phase provides completely beam-squint free performance as shown in the simulated in **Figure 3** below and is in agreement with [9].

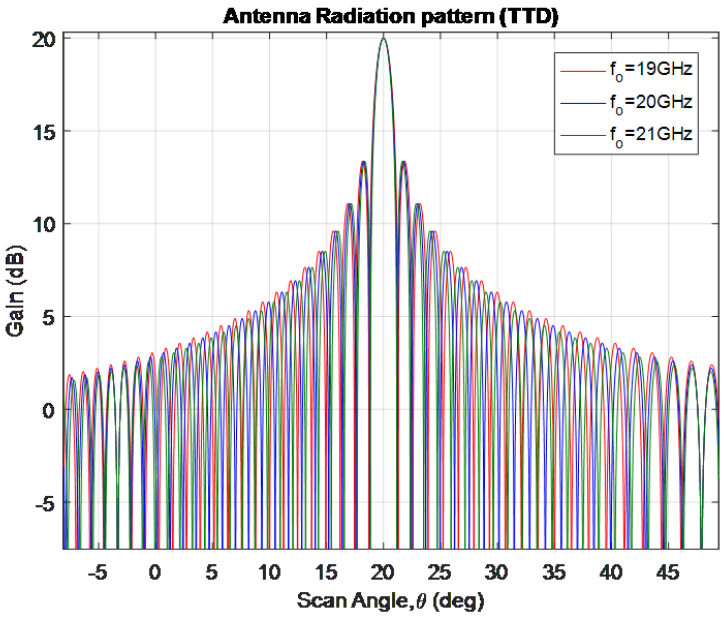

Figure 3 - Antenna Radiation pattern for True Time Delay showing no Beam squint

Figure 4 below shows a mathematical description of the True Time Delay Beamformer with both Delay and Phase compensation.

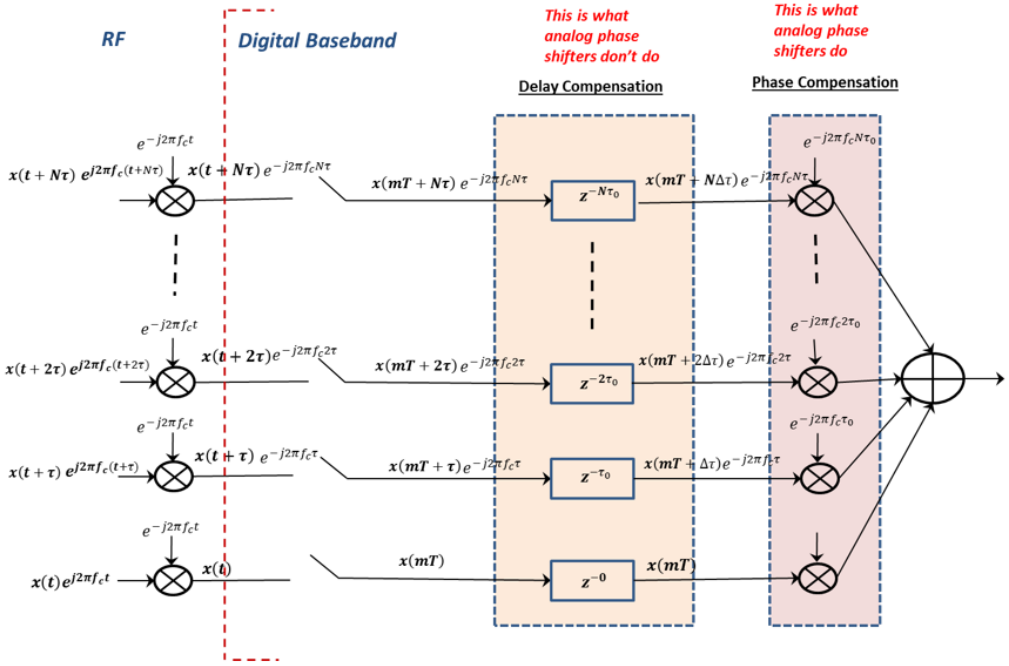

Figure 4 – Mathematical Description of True Time Delay Digital Beamformer

The signal received at each element in **Figure 4** is demodulated from RF to Baseband. For digital beamformer, the signal will then be digitized with processing shifting to discrete signal domain via A/D. This will be then followed by delay correction in the digital domain which corrects the delay to within certain residual delay error limit that allows [2.4] to hold for the wideband signal. Delay adjustment is followed by

phase correction (not necessarily in the same order) and the signals are then combined to produce a beamformed signal. Within the digital domain, the delay correction can be implemented with good precision and at a very low cost.

Equation [2.4] shows the relationship between the size of the antenna, the delay and the bandwidth of the baseband signal. **Table 1** below shows this relationship for the antenna of 1-D ULA with 100 elements and 200 elements (representative of 100 x 100 and 200 x 200 antenna array) for different carrier frequencies and signal bandwidths. The max delay in

Figure 5 shows the relationship between Signal Bandwidth and Antenna Size in 1-D to achieve a good performance (with little or no degradation due to beam squints). This only takes into the beam squint and no impacts to side-lobes of radiation pattern are considered due to uncompensated delay.

Table 1 is the delay between 1st element and the Nth element, where N=100 and 200 respectively. It can be noticed that for a signal with bandwidths 100 MHz and higher the max delay becomes a non-trivial fraction of the signal symbol duration and hence ignoring this delay correction in baseband signal will lead to degraded performance.

Figure 5 shows the relationship between Signal Bandwidth and Antenna Size in 1-D to achieve a good performance (with little or no degradation due to beam squints). This only takes into the beam squint and no impacts to side-lobes of radiation pattern are considered due to uncompensated delay.

Table 1- Max Delay across antenna vs. Bandwidth for different bands

Phased Array can operate with good performance ← | → ***TTD is essential for good performance***

Max Delay in Symbols, ULA -100 antenna elements, scan angle = 60°

f_c \ BW	1 MHz	10 MHz	25MHz	100MHz	200MHz	500MHz	1GHz	2GHz
12GHz	0.004	0.036	0.090	0.361	0.722	1.804	3.608	7.217
14GHz	0.003	0.031	0.077	0.309	0.619	1.546	3.093	6.186
20GHz	0.002	0.022	0.054	0.217	0.433	1.083	2.165	4.330
30GHz	0.001	0.014	0.036	0.144	0.289	0.722	1.443	2.887

Max Delay in Symbols, ULA -200 antenna elements, scan angle = 60°

f_c \ BW	1 MHz	10 MHz	25MHz	100MHz	200MHz	500MHz	1GHz	2GHz
12GHz	0.007	0.072	0.180	0.722	1.443	3.608	7.217	14.434
14GHz	0.006	0.062	0.155	0.619	1.237	3.093	6.186	12.372
20GHz	0.004	0.043	0.108	0.433	0.866	2.165	4.330	8.660
30GHz	0.003	0.029	0.072	0.289	0.577	1.443	2.887	5.774

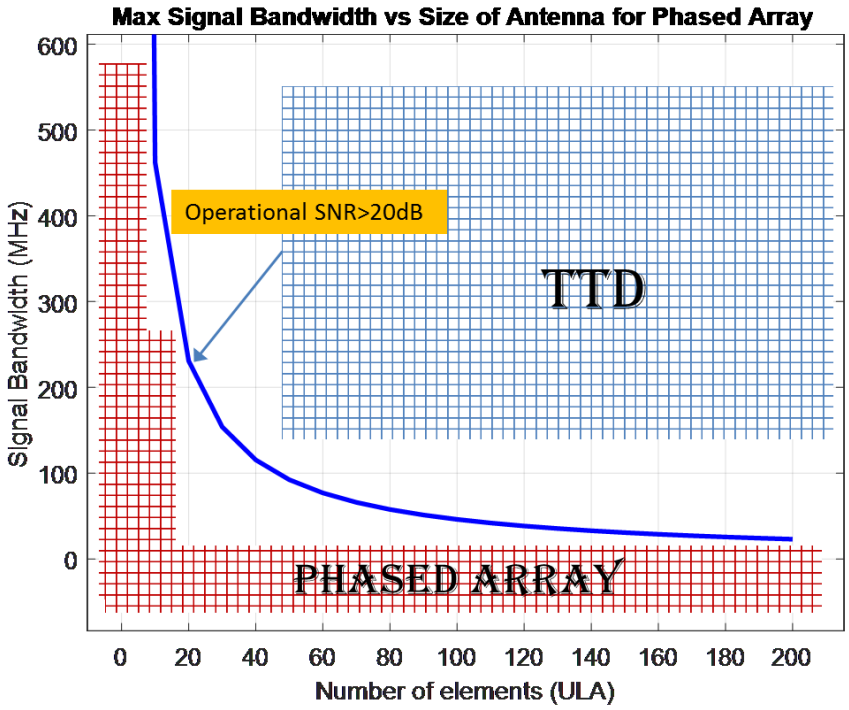

Figure 5 - Signal Bandwidth vs Antenna Size

3. Antenna Array Bandwidths

The antenna's bandwidth is a function of its effective aperture. For an array of antennas, the size of each patch and the distance between them influence the two main antenna characteristics

- Mutual Coupling
- Grating Lobes

These two aspects play an important role in defining the Antenna Bandwidth over which the efficiency of antenna can be maintained without significant loss. The high end of the frequency band is limited by the physical size of the antenna elements which must be placed close enough to avoid grating lobes. On the other hand, if the element spacing becomes too small ($d < \frac{\lambda}{2}$), then mutual coupling, which is the electromagnetic interaction between the elements, becomes quite pronounced. The mutual coupling can modify the array radiation pattern and can also modify the impedance of the antenna thereby impacting the matching characteristics of the antenna and reducing the antenna efficiency. Hence the BW of the antenna array for which the efficiency is high is to strike the right balance between Mutual Coupling and Grating Lobes.

The conditions for separation between elements to avoid grating lobes for particular scan angle θ_o is given as follows

$$d < \frac{\lambda}{1 + sin\theta_0} \qquad [3.1]$$

where d is the distance between the antenna elements

λ is the wavelength of the incident wave

Therefore for $\theta_0 = 90^0$, $d < \frac{\lambda}{2}$, which is the necessary condition to have no grating lobes within the visible region for the entire scanning range.

Consider the information signal to be a CW tone of frequency f_B, $x(t) = \exp(j2\pi f_B t)$, which is modulated by carrier f_c and sent over the air

The transmitted signal at the far region from the antenna array is shown as below

$$s(t) = \sum_{n=0}^{N-1} x(t + n\tau) e^{(j2\pi f_c t)} exp\left(\left(j2n\pi f_c(\tau - \tau_0)\right)\right)$$

where, $\tau_0 = \frac{\sin(\theta_0)}{2f_c}$ [3.2]

Substituting for the signal $x(t)$,

$$s(t) = x(t)e^{(j2\pi f_c t)} \sum_{n=0}^{N-1} exp\left(\left(j2n\pi(f_c + f_B)(\tau - \tau_0)\right)\right)$$

[3.3]

The Array Factor gain for a signal steered in a direction θ_0 in the expression above is

$$AF = \sum_{n=0}^{N-1} exp\left(\left(j2n\pi(1+\alpha) * 0.5 * (sin(\theta) - \sin(\theta_0))\right)\right)$$

where, $\alpha = \frac{f_B}{f_c}$

[3.4]

The equivalent antenna element distance due to CW tone gets altered from $d = 0.5\lambda_c$ to $(1+\alpha) * 0.5\lambda_c$. Radiation patterns for different values of α are given in **Figure 7**

Table 2 below captures the relations between α, d_{eq} and θ_0 to avoid grating lobes

Table 2 Relationship between scan angle, element spacing and $\boldsymbol{\alpha}$

$\boldsymbol{\theta_0}$	$\boldsymbol{d_{eq}/\lambda}$	$\alpha = (d_{eq}/0.5\lambda) - 1$
90	0.5	<<1
75	0.5087	1/58
60	0.5359	1/14
45	0.5858	1/6
30	0.6667	1/3
15	0.7944	< ½
0	1	1

Table 2 shows an interesting relationship between the CW tone frequency w.r.t carrier frequency, which would impact the grating lobes for a particular scan angle. This result can be extended to wideband signals with highest frequency f_B i.e. bandwidth $BW = f_B$, which will cause the formation of grating lobes and hence dissipate unwanted energy in the visible region thereby causing interference. The grating lobes can be avoided by absorbing the $(1+\alpha)$ term within interlement spacing i.e.

$$d = \frac{0.5\lambda_c}{(1+\alpha)} \quad [3.5]$$

but this could increase mutual coupling as the distance between elements are now less than $0.5\lambda_c$ as shown in **Figure 6**

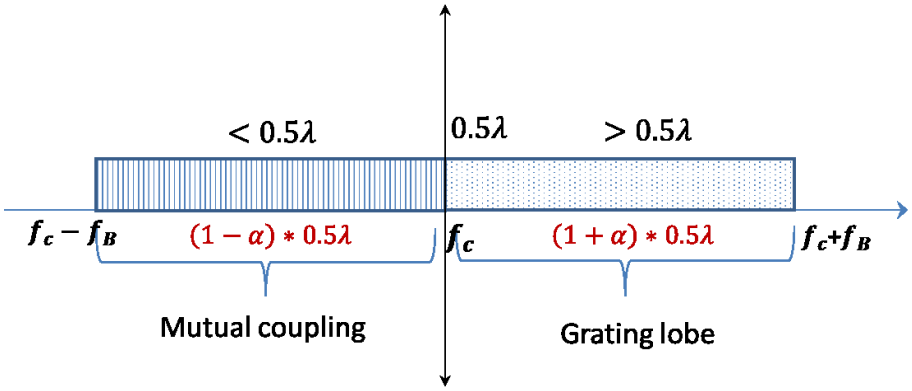

Figure 6- Mutual Coupling and Grating Lobe zones

Using the relationship between scan angle θ_0 and the ratio of the CW tone to the modulating carrier frequency (used to design the element spacing within array), α one can now derive the effective Antenna BW w.r.t. the scan angles.

Table 3- Bandwidth for different scan angles and frequencies

Bands	f_c (GHz)	Scan angle, θ_0	α	f_B (GHz)	BW (GHz)
Ku	12	75	1/58	0.207	0.414
		60	1/14	0.857	1.714
		45	1/6	2	4
	14	75	1/58	0.242	0.484
		60	1/14	1	2
		45	1/6	2.33	4.66
Ka	20	75	1/58	0.345	0.69
		60	1/14	1.429	2.858
		45	1/6	3.33	6.66
	30	75	1/58	0.517	1.034
		60	1/14	2.14	4.28
		45	1/6	5	10

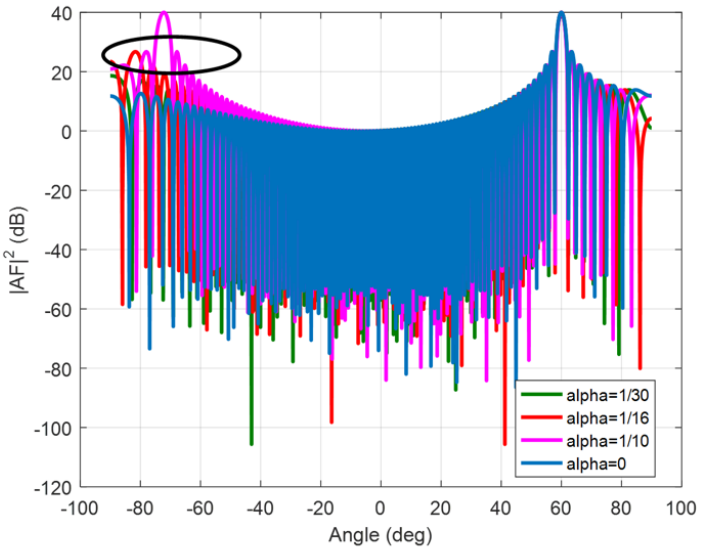

Figure 7- Antenna Array Radiation pattern for different α

4. Impairments

This section will analyze the impacts of RF impairments as well as Quantization Noise within the digital domain on the beamformer performance. It is also important to find out how much impairment the system can tolerate without noticeable impact on Tx and Rx performance, which in turn set out the minimum requirements that the calibration algorithms must meet. In particular, the impact of the following impairments on the beamformer array performance are discussed in this section:

- Random phase error
- Random gain error
- Phase noise
- Quantization noise

4.1. Random Phase Offset and Gain Imbalance

In this section, we analyze the impact of random phase offsets between elements on the beamformer radiation pattern. For simplicity, a tone input is assumed, however the results equally apply to any type of input. The phase offset may arise directly from different initial phases of the LO between different elements, or equivalently from relative time delays between the elements (due to any reason) can be represented as random phase offset between elements.

Assume that the random phase offset between the array elements can be modeled as a uniformly distributed random variable between $[0, \psi]$, $0 \leq \psi \leq 2\pi$, or equivalently $[-\psi/2, \psi/2]$, $0 \leq \psi \leq 2\pi$. It can be shown that, for a square NxN array, in the presence of uniformly distributed random phase offset, the expected value of the beamforming array factor as a function of off-axis angle θ is given by

$$E\{A(\theta)\} = \underbrace{\frac{\sin^2\left(\psi/2\right)}{\psi^2/}}_{\text{Scaling of main lobe}} PG^2(\theta)A_0(\theta) + \underbrace{PG^2(\theta)N^2\left|1-\frac{\sin^2\left(\psi/2\right)}{\psi^2/}\right|}_{\text{Spatial Noise Floor}} \quad [4.1]$$

where P is the transmit power per element, $G(\theta)$ denotes the patch antenna gain, and $A_0(\theta)$ denotes the ideal array factor without the impairments as a function of off-axis angle θ.

From [4.1], it is observed that the presence of random phase offset reduces the main lobe power and introduces a spatial noise floor that is independent from the off-axis angle. Note that similar results as expression [4.1] are available in literature (e.g. [7]), however, in those studies, only the impact on the main-lobe degradation is considered, but not the spatial noise component.

For small phase offset values, the scaling in the main lobe approaches to unity and the bias term goes to zero. On the other hand, as phase offset gets larger, the main lobe reduces and, in the limit, it goes to zero, when the phase offset is distributed over the full range from 0 to 360°. The bias term approaches to $A_0(0)/N^2$ in this case, (where $A_0(0)$ simply denotes the main lobe power in the ideal case), which is roughly given by $20*\log10(N)$ dB + antenna gain.

Figure 8 shows the EIRP vs. the off-axis angle with and without phase offset for uniform random phase offset in [0,90°] (or equivalently [-45,45°]). Simulation parameters are: Fc=30 GHz (Ka band), signal BW=200 MHz and the results shown are for 100x100 array. The simulation results are averaged over 1000 different runs. Also shown in the figure are the theoretical expected value as given by above, which shows excellent agreement between theory and simulations.

Figure 9 displays the reduction in the main lobe with respect to phase offset maximum value. In order to limit the degradation to less than 0.1 dB, the maximum relative phase offset should ideally be limited to < 30° which requires an online phase/delay calibration if the maximum relative phase offset/delay between elements likely to exceed 2.7 ps in Ka band (or 5.5 ps in Ku band). This equivalently means that the absolute phase error must remain less than ±15°. These results apply when there is no tapering. In case of tapering, requirements are more stringent, basically due to the more strict requirement on sidelobe level required in this case, as discussed in subsequent sections.

In the presence of uniformly distributed gain imbalance between [-a,a] dB, it can be shown that the array factor as a function of off-axis angle θ can be expressed:

$$E\{A(\theta)\} = \underbrace{\gamma}_{\text{Scaling}} P_{TX}G^2(\theta)A_0(\theta) + \underbrace{P_{TX}G^2(\theta)N^2(\eta-\gamma)}_{\text{Spatial Noise Floor}} \quad [4.2]$$

$$\eta = \frac{5}{a\log10}\left(10^{a/10}-10^{-a/10}\right), \eta \geq 1, \ \gamma = \left(\frac{10}{a\log10}\left(10^{a/20}-10^{-a/20}\right)\right)^2, \eta \geq \gamma \geq 1$$

where $A_0(\theta)$ denotes the ideal array factor without the impairments, N is the total number of antennas, P_{TX} is the transmit power and $G(\theta)$ denotes the patch antenna gain at the specific direction. As in the case of random phase offset, gain imbalance impacts the main lobe power as well as the off-axis emission levels due to presence of spatial noise floor caused by random gain offset. Note that since $\gamma \geq 1$, unlike phase offset case, the main-lobe power is not reduced but is amplified.

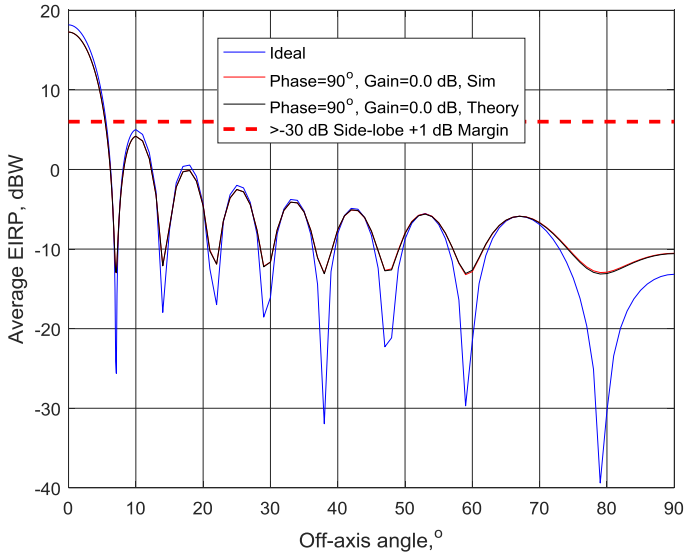

Figure 8 Off-axis EIRP (averaged over 1000 runs) in the presence of random phase offset (max 90°)

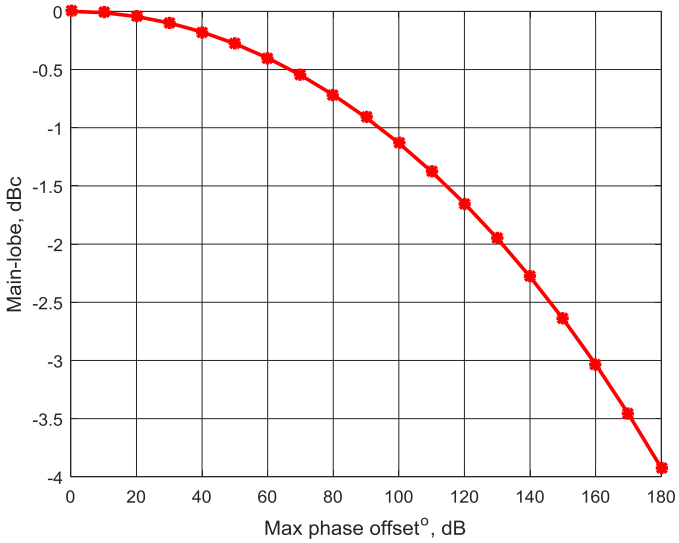

Figure 9 Main lobe power reduction vs max phase offset

For the co-existing gain and phase offset between array elements, in order to determine the maximum tolerable phase and gain offset values, the following requirements are established:

- {Probability of > 1 dB loss in main-lobe} should be < 0.01%
- No tapering: {Probability of side-lobe growth > 1 dB} should be < 0.01%
- Tapering: {Probability of side-lobe growth >2 dB} should be < 1%

The maximum tolerable impact of gain and phase offset levels are then analyzed via simulations. The phase offset distribution is uniform but the gain imbalance distribution is assumed to be Gaussian, which yields similar degradation as uniformly distributed gain imbalance case but may be more prevalent in practice. In the simulation, 16x1 array is assumed operating at Fc=14 GHz (Ku band) with signal BW=500 MHz. For tapering, Taylor window is used with 25 dB side-lobe suppression.

The worst-case performance is determined by tapering. If there is no tapering, in order to meet the requirements above, relative phase offset between elements should be limited to ±15° and gain imbalance should be kept below 0.5 dB. However, requirements become more stringent if tapering is applied. Table 4 below displays the simulation results with tapering. Boresight steering is assumed (i.e. 90° elevation) but the upper limits do equally apply for other steering angles as well.

Based on the simulation analysis, it can be concluded that, in order to meet the requirements, including the tapering case, the relative phase offset between elements should be limited to ±5° and gain imbalance should be kept below 0.2 dB.

Table 4 Impact of Uniform Phase offset/Gaussian Gain Imbalance (with tapering)

Probability of Side-Lobe Growth > 2 dB (Boresight, with tapering)							
Gain offset: σ_{dB} / Phase offset [-ΔΨ, ΔΨ°]	0	0.1	0.2	0.3	0.4	0.5	0.6
0	0%	0%	0%	0.01%	0.24%	1.55%	4.22%
5	0.54%	0.58%	1.03%	2.07%	3.87%	6.64%	10.7%
10	16.37%	17.53%	17.54%	18.65%	21.12%	24.15%	26.9%

4.2. Phase Noise

Phase noise is modeled as multiplicative colored random process with non-white temporal correlation. Figure 10 below shows the model for generation of non-white (a.k.a pink) phase noise from white noise process.

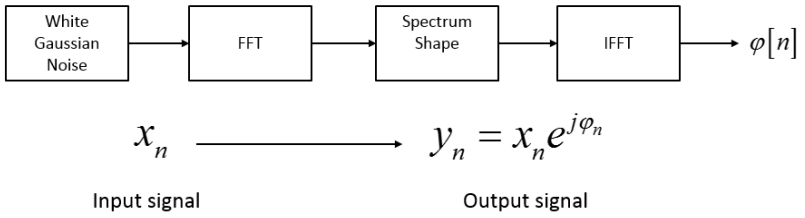

Figure 10 Phase noise modeling

In general, spectrum shaping is done according to the spot phase noise power spectral density (dBc/Hz) at different frequency offsets relative to LO carrier frequency. IPN (Integrated Phase Noise, dBc) for each frequency offset is then computed by integrating phase noise from that frequency to 1 GHz by using piece-wise linear approximation in log-frequency domain. Given the IPN, the RMS phase noise and corresponding RMS jitter in time-domain are expressed as:

$$\Phi_{RMS}{}^{o} = \left(\frac{180}{\pi}\right) 10^{\frac{IPN_{dBc}+3}{20}}, \tau_{RMS} = \frac{\Phi_{RMS}{}^{o}}{360 F_c}(\text{sec}) \qquad [4.3]$$

where F_c denotes the LO carrier frequency.

4.2.1. LO Distribution Model

Distribution of LO between the elements of the beamformer array has significant impact on the way that phase noise affects the antenna pattern and beamforming performance. In general, if all elements are fed by different LO, the resultant phase noise would be uncorrelated between the elements, and full array combining gain can be obtained which greatly improves the signal-to-phase noise ratio. On the other hand, the impact of phase noise is more severe on the radiation pattern (nulls and side-lobes) if the individual array elements are subject to uncorrelated phase noise. On the other hand, it is intuitively clear that if all elements share the same LO, there will not be any combining gain in phase noise SNR, however, there will be no negative impact on the radiation pattern either as every element will experience the same phase noise and relative phase difference due to phase noise between elements will always be zero.

In practice, there will be some grouping of elements that share the same LO. The elements in the same group would experience the same (i.e. fully correlated) phase noise, while the phase noise would be uncorrelated between the two elements that belong to different LO groups. Hence, in practice, the impact of phase noise on combined SNR and spatial emission pattern will be in between the two extremes mentioned in the above paragraph.

4.2.2. SNR of the Combined Signal

In the presence of phase noise, the combined signal in the steering direction is given by

$$y(t) = x(t)\sum_{n=1}^{N^2} e^{j\varphi_n(t)} \qquad [4.4]$$

where $\varphi_n(t)$ denotes the phase noise process for antenna element *n*, with zero-mean and variance $\sigma^2 = 10^{-IPN/10}$, where IPN denotes the integrated phase noise in dBc. This can be expressed in the following form:

$$y(t) = N^2 x(t) + \eta(t), \quad \eta(t) = x(t)\left(\sum_{n=1}^{N^2} e^{j\varphi_n(t)} - N^2\right) \qquad [4.5]$$

where the noise is decoupled from desired signal and becomes additive.

Now assume that the LO distribution is such that the N^2 elements are divided into equal sized groups, each consisting of K elements, and every element in the group shares the same LO, hence experiences the same phase noise, while phase noise is independent between the groups. In that case, assuming that $\mathrm{E}\{x(t)\}=0$, it can be shown that:

$$\begin{aligned} &E\{\eta(t)\} = 0, \\ &E\left\{|\eta(t)|^2\right\} = R_x(0)\left(N^2\left(K+N^2\right) + N^2\left(N^2-K\right)e^{-\sigma^2} - 2N^4 e^{-\sigma^2/2}\right) \end{aligned} \qquad [4.6]$$

Therefore, combined SNR (combined signal power in the steering direction to phase noise ratio) can be expressed as:

$$SNR = \frac{N^4 R_x(0)}{E\left\{|\eta(t)|^2\right\}} = \frac{1}{\left(e^{-\sigma^2} - 2e^{-\sigma^2/2} + 1\right) + N^{-2}K\left(1 - e^{-\sigma^2}\right)} \qquad [4.7]$$

For $\boldsymbol{\sigma^2 \ll 1}$, using the approximation $\boldsymbol{e^{-x} \approx 1 - x}$, the above expression can be rewritten as

$$\mathrm{SNR} \approx \frac{N^2}{K\sigma^2} \Rightarrow \mathrm{SNR}_{\mathrm{dB}} \approx 20\log_{10} N - 10\log_{10} K - \mathrm{IPN} \qquad [4.8]$$

Special cases:

- All elements use different LO hence experience different phase noise (K=1):

$$SNR = \left(\left(e^{-\sigma^2} - 2e^{-\sigma^2/2} + 1\right) + N^{-2}\left(1 - e^{-\sigma^2}\right)\right)^{-1}$$
$$\text{For } \sigma^2 << 1,\ SNR \approx \frac{N^2}{\sigma^2} \Rightarrow SNR_{\text{dB}} = 20\log_{10} N - IPN \qquad [4.9]$$

- All elements share the same LO hence experience the same phase noise (K= N^2):

$$SNR = \frac{1}{2\left(1 - e^{-\sigma^2/2}\right)}$$
$$\text{For } \sigma^2 << 1,\quad SNR \approx \frac{1}{\sigma^2} \Rightarrow SNR_{dB} = -IPN \qquad [4.10]$$

As can be seen from [4.9] and [4.10], when every element shares the same LO, there will be no combining gain in signal-to-phase noise ratio, while if every element is fed by different LO, full combining gain ($10\log_{10}N^2$=$20\log_{10}N$ dB) is achieved. Figure 11 below depicts the expected combining SNR gain for different LO distribution schemes for 16x16 array.

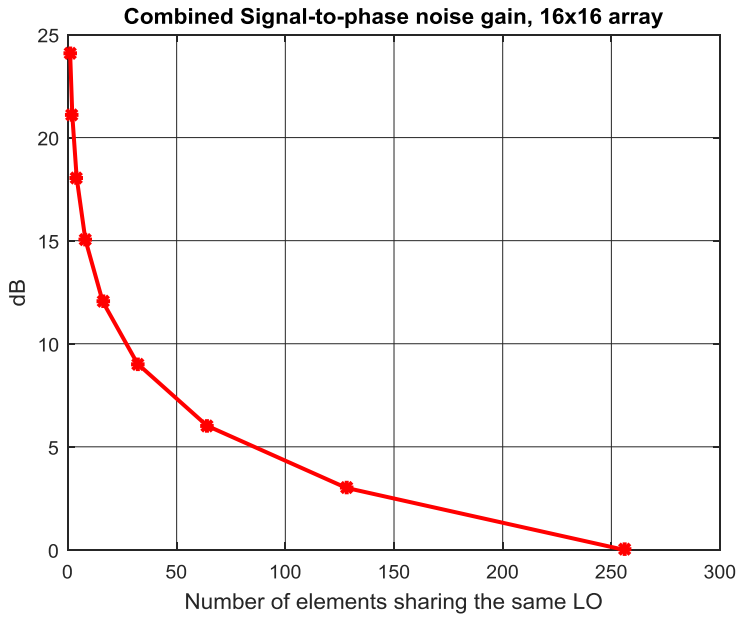

Figure 11 Combining gain (in the steering direction) in signal to phase noise ratio

4.3. Impact of Phase Noise and LO Distribution on Radiation Pattern

As mentioned before, while LO sharing is not good in terms of array gain in signal-to-phase noise ratio, it is better in terms of the impact on the radiation pattern (i.e. side-lobes, nulls etc).

In order to assess the impact of LO sharing and phase noise on the transmitted array pattern, a Matlab simulation is carried out with the following simulation parameters:

- Ku-band (Fc=14 GHz)

- Signal BW = 125 MHz
- 8x8 array
- Signal pulse shaping: RRC, with roll-off=0.05 (APSK-16 digital modulation)
- Steering: Boresight
- Phase noise IPN (from 10 Hz to 1 GHz): -12 dBc
- No tapering

Table 5 and **Figure 12** display the impact on array pattern in terms of main lobe loss, max side-lobe growth and max null growth for different group sizes, in which fully correlated case refers to single group and fully uncorrelated case denotes no grouping at all, whereas group sizes 8, 16 and 32 refer to 8, 4 and 2 groups of elements, each consists of 8, 16 and 32 elements, respectively. Also included in the plots is the fully uncorrelated case in which the IPN is computed from 100 Hz, as opposed to 10 Hz, which results in IPN=-17 dBc. The results suggest that:

- If phase noise per element is acceptable, i.e. no combining gain is needed, it may be advisable to share the LO as much as possible.
- If overall phase noise combining gain is desired, i.e. if phase noise per element (as it is) is a concern, then LO sharing should be avoided as much as possible.
- In order to obtain some gain in signal-to-phase noise ratio without too much impacting the radiation pattern, it is advisable to use 2 equal-sized groups which can offer up-to 3 dB gain in SNR. **Figure 13** depicts an example LO distribution configuration, using 2 LO's, each drive 32 elements.

Table 5 Phase Noise and LO Distribution impact (8x8 array, Bore-sight, No tapering)

Configuration	IPN range	IPN, dBc	Combined SNR, dB (SNR Gain in dB)	Radiation pattern impact		
				Main lobe loss, dB	Max Side-lobe growth, dB	Null growth, dB (max)
All 64 uncorrelated	10 Hz-1 GHz	-11.7	6.3 (18.0)	0.3	0.2	27
8 groups x 8 elements	10 Hz-1 GHz	-11.7	-2.7 (9.0)	0.3	0.7	30
4 groups x 16 elements	10 Hz-1 GHz	-11.7	-5.9 (5.8)	0.2	0.7	32
2 groups x 32 elements	10 Hz-1 GHz	-11.7	-8.9 (2.8)	0.1	0.3	15
All 64 correlated	10 Hz-1 GHz	-11.7	-11.7 (0.0)	0	0	0
All 64 uncorrelated	100 Hz- 1 GHz	-13.5	4.5 (18.0)	0.2	0	25
All 64 correlated	100 Hz- 1 GHz	-13.5	-13.5 (0.0)	0	0	0

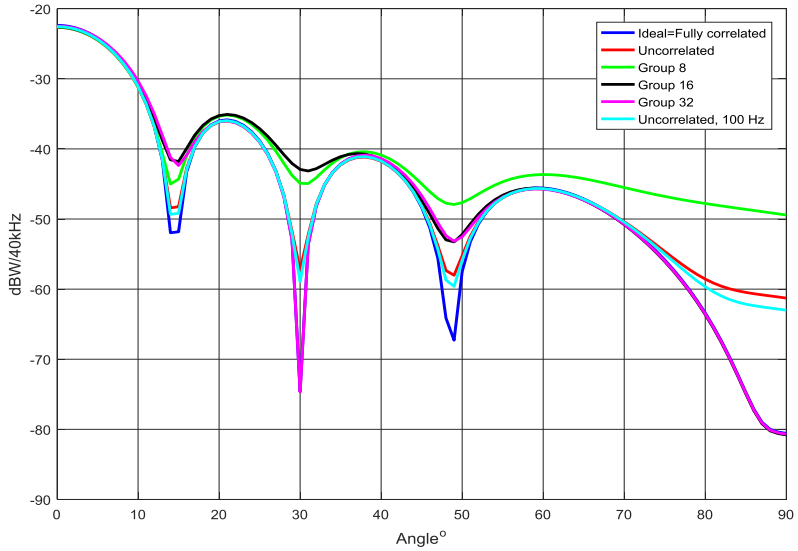

Figure 12 Phase Noise and LO Distribution impact on Tx Array Pattern (8x8 array, Bore-sight, No tapering)

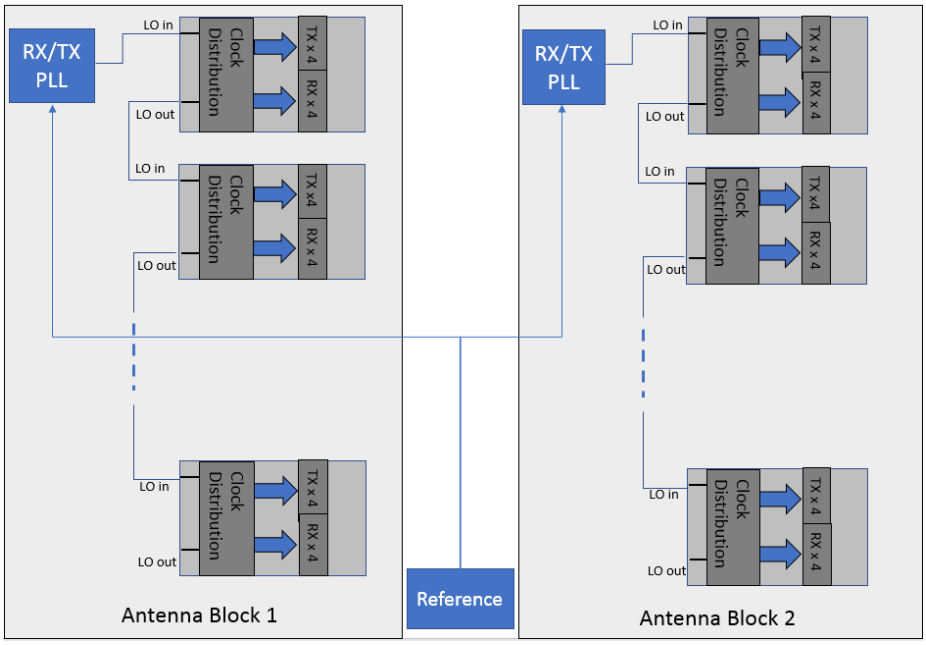

Figure 13 LO distribution example

4.4. Fixed-point implementation and SQNR

Quantization noise is an important factor in digital beamforming implementation which may have an impact on the array gain and off-axis emission pattern [8]. This section is devoted to the analysis of fixed-point implementation impacts on the beamformer performance. The main metric is the Signal-to-Quantization

Noise ratio (SQNR) per chain (i.e. antenna) and after combining. The impact of quantization noise to the off-axis emission is discussed in the next section.

Note that the quantization noise is in general not strongly correlated between elements if steering is applied to any direction other than boresight, since each element would see a slightly delayed version of the input signal. For small delays and for boresight where there is no delay, quantization noise at each element would be correlated hence combining gain would not apply to SQNR at the combiner output.

SQNR at the input of the beam-former is determined by the input signal bit-width (Q) and dynamic range, which depends on the peak-to-average power ratio (PAPR), and is given by:

$$\mathrm{SQNR}_{\mathrm{dB}} = \left(20\log_{10} 2\right)(Q-1) - 10\log_{10}\left(1/6\right) - \mathrm{PAPR}_{\mathrm{dB}} \approx 6.02Q + 1.78 - \mathrm{PAPR}_{\mathrm{dB}} \qquad [4.11]$$

which is a well-known result stating that SQNR is improved by approximately 6 dB for each additional bit.

Within the digital beamformer, the signal is multiplied by a complex factor that represents the beam-forming phase and tapering weight, which is denoted by complex number w. The resultant signal is then up-sampled to the DAC sampling rate via a series of interpolating filters. It can be shown that by selecting the complex coefficient bit-width at least 2 bits larger than signal bit-width (i.e. $\geq Q$+2), additional penalty due to complex multiplication and interpolation filtering stages can be avoided. However, application of tapering in general may have a considerably negative impact on SQNR since it may reduce the dynamic range of the signal when the tapering weight is less than unity. At the final stage, the signal is scaled back to the DAC bit-width (Q_{DAC}), and additional quantization noise is added by the DAC itself, which is captured by the ENOB (Equivalent Number of Bits) of the DAC, which is in general less than the DAC bit-width. It can then be shown that, the SQNR at the output of Tx for one element can be approximated by

$$\mathrm{SQNR}_{\mathrm{dB}} = 6.02(ENOB-1) + 20\log_{10}|w| - \mathrm{PAPR}_{\mathrm{dB}} - 10\log_{10}\left(4^{Q_{DAC}-Q}\left(\frac{|w|^2}{6}+\frac{1}{6}\right)+\frac{1}{6}\right) \qquad [4.12]$$

For the SQNR of the combined signal at the steering direction, it is clear that the quantization noise, which is present at the input signal will be fully-correlated between elements since the identical signal is fed to all elements hence combining gain cannot be achieved. However, for the other quantization noise sources (like beam-forming, tapering and DAC), the quantization noise is uncorrelated between elements and therefore the noise is combined incoherently which greatly suppresses the impact of quantization noise from other sources within the digital beam-former. It can be shown that, provided that $ENOB \geq Q$-3, the $SQNR$ for the combined signal is given approximately by:

$$\mathrm{SQNR}_{combined} \sim 6.02\mathrm{Q} - \mathrm{PAPR}_{\mathrm{dB}} - 10\log_{10}\left(1+\frac{1}{N}\right) + 1.78\ [\mathrm{dB}] \qquad [4.13]$$

which depends only on N (the number of array elements) and the input bit-width (Q), provided that DAC $ENOB$ is not worse than Q-3.

Figure 14 below depicts the SQNR per array element for tapering case, in which different gains are applied to each antenna, which effectively makes the signal dynamic range different for each element. Input bit-width is 8 and DAC bit-width is 7 (DAC ENOB is assumed to be as DAC bit-width). The input signal is an RRC-signal with 5% roll-off factor, modulated with random 16-APSK symbols and has a PAPR of ~ 7.5 dB. Hence, the input SQNR is given approximately by 42 dB. It is seen that although the per element SQNR varies because of differing tapering weight and may considerably be less than input SQNR, the combined SQNR is ~41.7 dB, which is almost the same as input SQNR, as expected from [4.13].

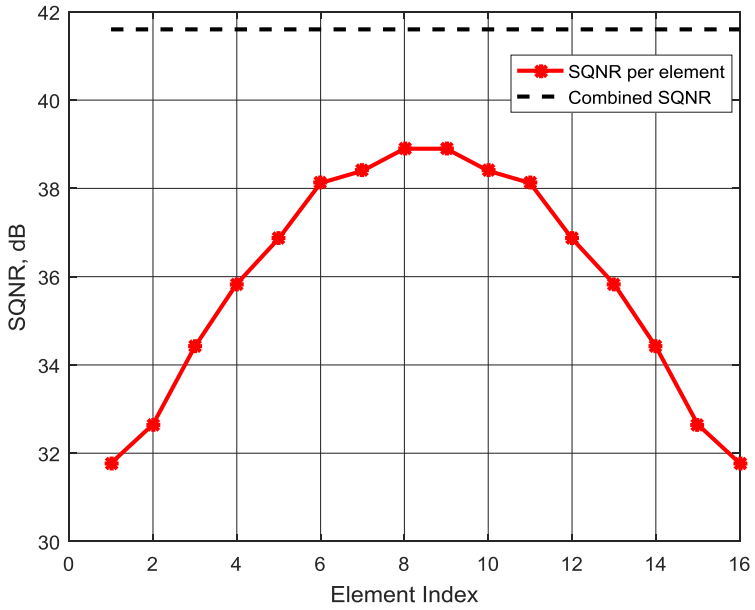

Figure 14 SQNR distribution in tapering case (16x1 array), Tapering: Taylor window

4.4.1. Impact on Emission Pattern

In order to assess the impact of the quantization noise on the radiation pattern, a simulation is run for 16x1 array, with and without tapering, assuming 8-bit input and 7-bit DAC. The performance loss due to fixed-point compared to full floating-point model is minimal if tapering is not applied (i.e. |w|=1 for all elements), the only slight impact is ~0.3 dB growth in the null-points. However, with tapering, the performance impact due to fixed-point becomes noticeable. As seen from **Figure 15** below, ~0.5 dB growth in side-lobes are observed. More importantly, up-to 14-15 dB degradation (growth) is seen in the null-points. However, almost no loss in SNR is observed in the steering direction compared to floating-point.

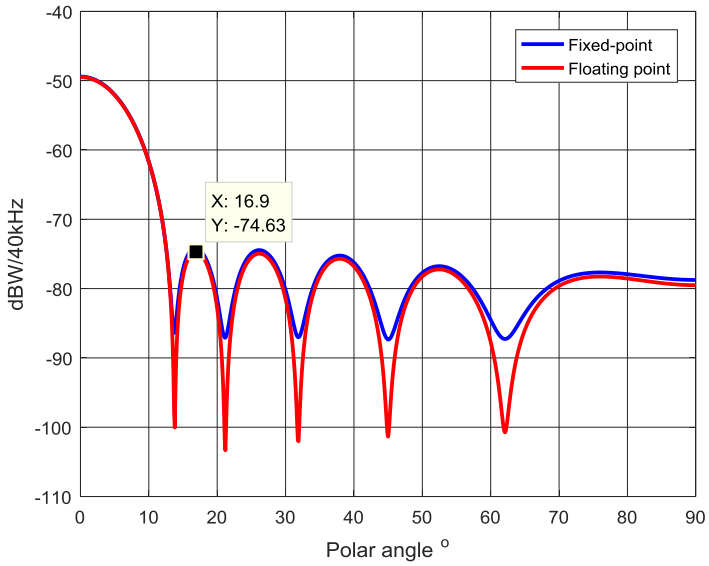

Figure 15 Radiation pattern, 16x1 array, 8-bit input, 7-bit DAC (ENOB) with Taylor window tapering

5. Calibration for Digital Beamformer

Following the discussion on digital beamformer calibration requirements from [1], in this section we delve further into the following aspects of calibration.

- System model for sources of phase and delay errors introduced within a beamformer array
- RF front end response calibration

5.1. Phase and Delay Modelling for Calibration

Understanding the sources of phase and delay errors within a beamformer array is crucial for calibration and therefore successful synchronization of the system. To the best of the authors' knowledge, a complete system model of the sources of delay and phase errors within a beamformer array has not been reported in the previous publications [2,3,4,5,6], and is therefore presented here.

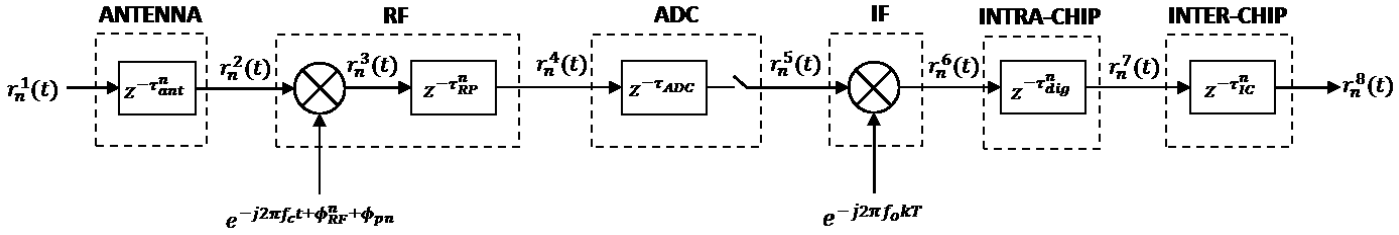

Figure 16 Internal Sources of Phase and Delay Errors at element n

Figure 16 depicts the various sources of delay and phase error within analogue and digital domains considered at a single chain of the beamforming array. The received signal at the input of the beamformer chain can be modelled in the complex domain as shown in equation 5.1 below.

$$r_n^1(t) = x(t)e^{j2\pi(f_c+f_o)(t)} \quad [5.1]$$

where,
f_c: Carrier frequency
f_0: Intermediate frequency

In the analogue domain, the antenna will introduce a delay denoted as $\boldsymbol{\tau_{ant}}$. Due to the part-to-part variation and non-linearity of the analog components, it is expected that there will be a unique phase error introduced within the RF device on each chain, denoted as $\boldsymbol{\phi_{RF}^n}$. Additionally, the phase noise introduced by the local oscillator will contribute to the phase error, denoted as $\boldsymbol{\phi_{pn}}$. Furthermore, the RF device is expected to introduce a delay to the signal due to the random PLL settling times across different beamformer chains. With respect to a common time reference, the PLL settling time delay on each chain is shown as $\boldsymbol{\tau_{RP}^n}$. It is important to note that the PLL lock-time delay modelling should take into consideration whether an integer or fractional PLL will be chosen for the system under design, and whether the PLL synchronization can be achieved across elements to avoid this error contribution.

The signal model after the addition of the combined delay and phase error contributions in the analogue domain is represented by equation 5.2 below.

$$r_n^4(t) = x(t - n\tau_{ant} - \tau_{RP}^n)\, e^{j2\pi(f_o(t-\tau_{RP}^n)-(f_c+f_o)n\tau_{ant})+\phi_{RF}^n+\phi_{pn}} \quad [5.2]$$

Following the analogue stage, the signal will be sampled within the ADC block which will have a delay contribution in the digital domain, denoted as $\boldsymbol{\tau_{ADC}^n}$.Note that any further phase noise introduced at this stage is ignored and without loss of generality, absorbed into the analogue phase noise figure mentioned

earlier. The signal will next be down-converted to baseband from the IF frequency. It is expected that there will be small differences in the routing delays within the digital logic amongst the different digital beamformer chains. This delay contribution is represented as $\boldsymbol{\tau_{dig}^{n}}$. Within a system of multiple digital beamformer chips, a further routing delay parameter, $\boldsymbol{\tau_{IC}^{n}}$, representing the delay within the multi-chip framework for the signal to reach different chips is also taken into consideration. Equation [5.3] represents the final form of the signal after the delay and phase error contributions in the digital domain.

$$r_n^8(t) = \left[x\left(kT - n\tau_{ant} - \tau_{RP}^n - \tau_{ADC}^n - \tau_{dig}^n - \tau_{IC}^n\right)\right] e^{j2\pi(f_o(-\tau_{ADC}^n - \tau_{RP}^n) - (f_c+f_o)n\tau_{ant}) + \phi_{RF}^n + \phi_{pn}}$$

[5.3]

From equation [5.3], the total delay error τ_{total}, and the total phase error φ_{total}within the signal can be extracted as:

$$\tau_{total} = -n\tau_{ant} - \tau_{RP}^n - \tau_{ADC}^n - \tau_{dig}^n - \tau_{IC}^n$$

[5.4]

$$\varphi_{total} = 2\pi(f_o(-\tau_{ADC}^n - \tau_{RP}^n) - (f_c + f_o)n\tau_{ant}) + \phi_{RF}^n + \phi_{pn}$$

[5.5]

It follows from equations [5.4] and [5.5] that to achieve phase and delay calibration, the following performance specification requirements must be satisfied:

$$-n\tau_{ant} - \tau_{RP}^n - \tau_{ADC}^n - \tau_{dig}^n + \hat{\tau}_n^D - \tau_{IC}^n \leq \tau_{delay}^{spec}$$

[5.6]

$$2\pi(f_o(-\tau_{ADC}^n - \tau_{RP}^n) - (f_c + f_o)n\tau_{ant}) + \phi_{RF}^n + \phi_{pn} \leq \theta_{phase}^{spec}$$

[5.7]

$$\left(f_o \Big/ (f_c + f_o)\right)(-\tau_{ADC}^n - \tau_{RP}^n) - n\tau_{ant} + \frac{\left(\phi_{RF}^n + \phi_{pn}\right)}{2\pi(f_c + f_o)} \leq \tau_{phase}^{spec}$$

[5.8]

where,

τ_{delay}^{spec}: minimum delay that can be tolerated

θ_{phase}^{spec}: minimum phase error that can be tolerated

τ_{phase}^{spec}: minimum delay derived from the minimum phase error tolerated

A cumulative delay and phase error estimation within specification limits is expected to suffice for most practical system calibration purposes. However, it is predicted that when a satisfactory beamforming array synchronization performance is not met, a finer break-down and control of each contribution of error will be required. In such cases system modelling must be assisted with laboratory characterization of isolated modules to understand how to calibrate and compensate for the errors at various stages via separate system parameters.

5.2. RF Front End Equalizer

In a beamforming array with multiple RF elements, it is evident that RFFE filter response will have a varying droop across different elements which will affect both the transmission pattern and the receiver combiner performance. To correct for this impairment, the RFFE response may be required to be equalized on each one of the beamformer chains particularly for a wideband signal. One of the advantages of digital

beamformer is the ability to equalize (for Rx) or pre-equalize (for Tx) the signal for each chain to achieve as close to possible distortion-less ideal beamforming gain at each frequency of the signal, thereby reducing the burden on RFIC design.

In practice, the equalizer filter can be derived during the offline calibration stage for RFFE responses observed over different temperatures. The derived equalizer taps can then be tabulated and stored in memory to be used in online mode. The equalizer derivation steps are shown in **Figure 17** below.

.

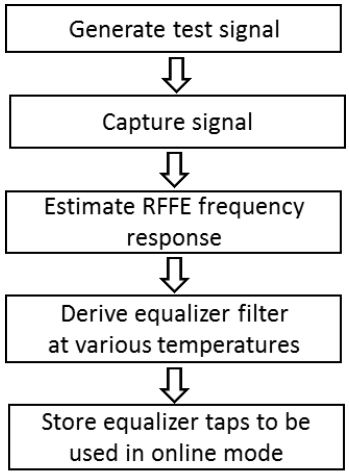

Figure 17 Equalizer Taps Derivation Steps

The digital design allows for a straight forward way of defining and implementing an equalizer filter following these steps for both the Rx path and as a pre-equalizer on the Tx path.

6. Conclusion

In this paper, we show the need for True Time Delay for a squint-free wideband active scanning antenna and present the simplicity with which digital beamforming can be used to implement it. We then consider the challenge of bandwidths for such an antenna with respect to balancing the grating lobes and mutual coupling to achieve the desired scan range. As part of this analysis we showed the relationship between antenna spacing and its impact on grating lobe. A wideband signal could potentially have part of its signal impacted by grating lobe and part of it by mutual coupling. Next, the paper shows the impacts of some analog and digital impairments such as random phase, gain, phase noise and quantization noise. These are important inputs for an overall design of an electronic scanning digital beamformer with respect to trading off complexity with performance requirements. We concluded the paper with a model demonstrating various sources of delay and phase misalignments that need to be calibrated to maintain tight synchronization for digital beamforming (some of it is relevant to analog beamformers as well) to provide full coherent combining gain at different scan angles. The relative amplitude variations across different frequencies for different RF front-end chains corresponding to different antenna elements can lead to beamformer gain being variable across frequencies. This can be reduced by using an equalizer or pre-equalizer in digital implementation relaxing the RFIC design constraints for front-end response (baseband filter, mixer, LNA and PA). The equalizer coefficients can be determined by factory calibration.

With recent advances in silicon technologies and availability of high speed ADCs and DACs, digital beamforming is overcoming the power and complexity barrier. This is paving the path for unlocking digital beamformer's full potential that can address the future needs of tracking antennas for high throughput satellite communications with cost advantage offered by silicon economics.

7. References

[1] Rainish, Doron, Freedman, Avraham, “Low Cost Digital Beamforming Array Structure and Architecture”, *22nd Ka and Broadband Communications Conference,*Cleveland, Ohio, October 17 - 20, 2016.

[2] Liang, G., Gong, W.B.,Liu,H.J., Yu,J.P.,”Development of 61-Channel Digital Beam-Forming (DBF) Transmitter Array for Mobile Satellite Communication”, *Progress In Electromagnetics Research*, PIER 97,177-195,2009.

[3] Lees,M.L.,“Digital beamforming calibration for FMCW radar”, *IEEE Transactions on Aerospace and Electronic Systems*,Volume: 25, Issue: 2, Mar 1989.

[4] Hu, Song, Hing, Gu, Jian, Wang,“Antenna Calibration and Digital Beam Forming Technique of the Digital Array Radar”, *2013 IEEE International Conference on Signal Processing, Communication and Computing (ICSPCC 2013)*,2013.

[5] Hampson, G.A.,Smolders, A.B., “A Fast and Accurate Scheme for Calibration of Active Phased-Array Antennas”, *IEEE Antennas and Propagation Society International Symposium*, 1999.

[6] K.M. Lee, R.S.Chu and S.C. Liu, “A built-in performance-monitoring/fault isolation and correction (PM/FIC), System for active phased-array antennas”, *IEEE Transactions on Antennas & Propagation,* AP-41, 1993, p. 1530-1540.

[7] Bakr O.M., Johnson M., “Impact of Phase and Amplitude Errors on Array Performance”, *Technical Report No UCB/EECS-2009-1*, University of California at Berkeley, Jan 2009

[8] Salim, T., Devlin, J., Whittington, J., “Quantization Analysis for Reconfigurable Phased Array Beamforming”, *International Symposium on Antennas and Propagation, ISAP2006*, p1-5.

[9] Longbrake, M., “Quantization Analysis for Reconfigurable Phased Array Beamforming”, *Aerospace and Electronics Conference (NAECON), IEEE National, 2012*

[10] M. I. Skolnik, Introduction to Radar Systems, 3rd ed. New York, NY: McGraw-Hill, 2001.

[11] A.F. Molisch: *Wireless Communications*, John Wiley and Sons. 2nd ed. 2011